Distal axonopathy in peripheral nerves of PMP22-mutant mice.

Sancho, S ; Magyar, J P ; Aguzzi, Adriano ; Suter, Ueli

Abstract: A partial duplication of chromosome 17 is associated with Charcot-Marie-Tooth disease type 1A (CMT1A), a demyelinating peripheral neuropathy that causes progressive distal muscle atrophy and sensory impairment. Trisomic expression of peripheral myelin protein 22 (PMP22) whose gene is contained within the duplicated region is considered to be responsible for the disease. By using recombinant gene technology in rodents, we had demonstrated previously that PMP22 is sensitive to gene dosage. Homozygous PMP22 knockout (PMP22(0/0)) mice and transgenic animals carrying additional copies of the PMP22 gene develop distinct peripheral polyneuropathies. We have now performed a detailed morphometrical analysis of the L3 roots, quadriceps and saphenous nerves of these PMP22-mutant mice to study whether the myelin and potential axonal deficits are evenly distributed. The L3 roots and the peripheral nerves were chosen as representatives of the proximal and distal segments of the peripheral nervous system. When the roots were compared with the peripheral nerves, myelin deficiencies appeared more severe at the radicular levels, in particular the ventral roots. Decreased numbers of large calibre axons were a prominent feature in the motor branches of both strains of PMP22-mutant mice, and these axonal deficits were more severe distally. Active axonal damage was only observed in the nerves of PMP22(0/0) mice. Despite the distinct effects on myelination and the Schwann cell phenotype that characterize the neuropathies of PMP22-mutant mice, both strains develop a distally accentuated axonopathy as a common disease mechanism which is likely to be responsible for the neurological deficits.

DOI: https://doi.org/10.1093/brain/122.8.1563

Brain (1999), **122,** 1563–1577

Distal axonopathy in peripheral nerves of *PMP22*-mutant mice

Sara Sancho,[1] Josef P. Magyar,[1] Adriano Aguzzi[2] and Ueli Suter[1]

[1]*Department of Cell Biology, Swiss Federal Institute of Technology and* [2]*Institute of Neuropathology, University Hospital of Zurich, Zurich, Switzerland*

Correspondence to: Professor Dr Ueli Suter, Institute of Cell Biology, Swiss Federal Institute of Technology, ETH-Hoenggerberg, CH-8093 Zurich, Switzerland
E-mail: usuter@cell.biol.ethz.ch

Summary

A partial duplication of chromosome 17 is associated with Charcot–Marie–Tooth disease type 1A (CMT1A), a demyelinating peripheral neuropathy that causes progressive distal muscle atrophy and sensory impairment. Trisomic expression of peripheral myelin protein 22 (PMP22) whose gene is contained within the duplicated region is considered to be responsible for the disease. By using recombinant gene technology in rodents, we had demonstrated previously that PMP22 is sensitive to gene dosage. Homozygous *PMP22* knockout (*PMP22*$^{0/0}$) mice and transgenic animals carrying additional copies of the *PMP22* gene develop distinct peripheral polyneuropathies. We have now performed a detailed morphometrical analysis of the L3 roots, quadriceps and saphenous nerves of these *PMP22*-mutant mice to study whether the myelin and potential axonal deficits are evenly distributed. The L3 roots and the peripheral nerves were chosen as representatives of the proximal and distal segments of the peripheral nervous system. When the roots were compared with the peripheral nerves, myelin deficiencies appeared more severe at the radicular levels, in particular the ventral roots. Decreased numbers of large calibre axons were a prominent feature in the motor branches of both strains of *PMP22*-mutant mice, and these axonal deficits were more severe distally. Active axonal damage was only observed in the nerves of *PMP22*$^{0/0}$ mice. Despite the distinct effects on myelination and the Schwann cell phenotype that characterize the neuropathies of *PMP22*-mutant mice, both strains develop a distally accentuated axonopathy as a common disease mechanism which is likely to be responsible for the neurological deficits.

Keywords: Charcot–Marie–Tooth disease; peripheral myelin protein 22; knockout mice; transgenic mice; axonal atrophy

Abbreviations: CMT = Charcot–Marie–Tooth disease; Cx32 = connexin32; HMSN = hereditary motor and sensory neuropathy; HNPP = hereditary neuropathy with liability to pressure palsies; NF = neurofilaments; PLP = proteolipid protein; PMP22 = peripheral myelin protein 22; P_0 = protein zero; *Tr* = *Trembler*

Introduction

The syndrome of peroneal muscular atrophy or Charcot–Marie–Tooth (CMT) disease is one of the most frequent inherited causes of neurological disability. Although initially considered to be a single clinical entity, Dyck and Lambert (Dyck and Lambert 1968*a*, *b*) established the heterogeneity of the syndrome on the basis of combined clinical, genetic, electrophysiological and nerve biopsy findings. Later, genetic studies substantiated that CMT disease encompasses several distinct peripheral neuropathies (reviewed by Patel and Lupski, 1994; Harding, 1995; Suter and Snipes, 1995; De Jonghe *et al*., 1997). The demyelinating form of CMT, also known as hereditary motor and sensory neuropathy (HMSN) type I, can be inherited as an autosomal dominant, X-linked or autosomal recessive trait (Dyck *et al*., 1993), and the most commonly found autosomal dominant CMT1 loci have been mapped to chromosome 17 (CMT1A) and chromosome 1 (CMT1B).

By far the most frequent cause of HMSN I (~70%) is a 1.5 Mb duplication in the chromosomal region 17p11.2 (Wise *et al*., 1993; Nelis *et al*., 1996) containing the *peripheral myelin protein 22* (*PMP22*) gene which encodes a 22 kDa membrane glycoprotein located in compact myelin of peripheral nerves (reviewed by Naef and Suter, 1998). Mutations in the murine *PMP22* gene are responsible for the naturally occurring CMT mouse models *Trembler* (*Tr*) and *Trembler-Jackson* (*Tr-J*) which initially implicated *PMP22* as the critical gene within the CMT1A duplication (Suter *et al*., 1992*a, b*). Furthermore, PMP22 point mutations have also been found in some rare cases of familial CMT1A without the usual chromosomal duplication and in the severe

childhood neuropathy Dejerine–Sottas syndrome (reviewed by De Jonghe *et al*., 1997). Since the *PMP22* gene is not disrupted by the CMT1A duplication (Matsunami *et al*., 1992; Patel *et al.,* 1992; Timmermann *et al*., 1992; Valentijn *et al*., 1992) and PMP22 is also not mutated in these patients (Warner *et al*., 1996), a gene-dosage effect has been suggested as the responsible disease mechanism. The observation that homozygous CMT1A duplication patients are often more affected than heterozygous relatives supports this hypothesis (Lupski *et al*., 1991; Kaku *et al*., 1993; LeGuern *et al*., 1997). Additional evidence for the dosage sensitivity of PMP22 was obtained when the corresponding 1.5 Mb deletion was identified in patients with hereditary neuropathy with liability to pressure palsies (HNPP) (Chance *et al*., 1993), consistent with the finding of three PMP22 mutations leading to presumed null alleles in familial HNPP (Nicholson *et al*., 1994; Bort *et al*., 1997; Young *et al*., 1997).

Clinically, CMT1A due to increased PMP22 gene dosage is usually a relatively benign condition, most commonly with an onset in the first or second decade, and shows progression throughout life. Although variability is observed, even within the same family, most patients have classical CMT, alone or associated with additional symptoms (Birouk *et al*., 1997; Thomas *et al*., 1997). The clinical phenotype includes a distal nerve length-related neuropathy affecting the lower limbs to a greater extent than the upper limbs, and motor function to a greater extent than sensory function. All sensory modalities, but in particular proprioception, can be affected. A high proportion of patients develop foot deformities, such as pes cavus and equinovarus. With disease progression, more proximal muscles also get involved. However, neurological deficits remain generally more prominent distally. Reduced nerve conduction velocity of both motor and sensory fibres is a regular finding. Histologically, a progressive demyelination of peripheral nerves is associated with Schwann cell hyperplasia, leading to the characteristic formation of onion bulb structures (Thomas *et al*., 1997).

To prove that indeed *PMP22* is the dosage-sensitive gene in the CMT1A duplication and to provide accurate animal models, transgenic mice and rats have been generated (Adlkofer *et al*., 1995, 1997; Huxley *et al.,* 1996, 1998; Magyar *et al*., 1996; Sereda *et al*., 1996). Homozygous PMP22 knockout (*PMP22*$^{0/0}$) mice develop a severe polyneuropathy with electrophysiological abnormalities typical of a myelin disorder. In the early post-natal period, the lack of PMP22 results in delayed myelin formation and focal hypermyelination (tomacula). Tomacula in *PMP22*$^{0/0}$ nerves have been considered unstable structures because myelin degeneration rapidly ensues and Schwann cell onion bulbs develop resulting in a demyelinating neuropathy resembling CMT1 (Adlkofer *et al*., 1995). In contrast, heterozygous PMP22 knockout (*PMP22*$^{+/0}$) mice develop pathological features reminiscent of HNPP in agreement with the corresponding genotypes (Adlkofer *et al*., 1997). Transgenic rats and mice with low numbers of additional copies of the *PMP22* gene develop a neuropathy that closely mimics the pathological features of CMT1A patients. The nerves of these animals show features of a demyelinating neuropathy with remyelination and the formation of onion bulb structures (Huxley *et al.,* 1996, 1998; Sereda *et al*., 1996). Severely increased *PMP22* gene dosage results in a strongly dysmyelinated disorder resembling congenital hypomyelination both in rats and mice (Huxley *et al.,* 1996, 1998; Magyar *et al*., 1996; Sereda *et al*., 1996). Thus, these transgenic animals together with the natural mouse mutants *Tr*, *Tr-J* and *Trembler PMP22*^{Ncnp} (*Tr-Ncnp*) (Suh *et al*., 1997) have revealed that PMP22 is involved in early steps of myelinogenesis, the determination of myelin thickness and the maintenance of myelin and axons of the PNS (reviewed by Naef and Suter, 1998).

In this report, we performed a systematic morphometric analysis of peripheral nerves of *PMP22*-mutant mice either lacking PMP22 or carrying elevated copy numbers of the *PMP22* gene, in order to evaluate the mechanisms resulting in the observed neuropathies. In particular, given the distally more pronounced symptoms in CMT1 patients, we wanted to compare the pathological lesions affecting axons and myelin between proximal and distal segments of a given nerve. In addition, we were interested in assessing whether the pathological process affects motor and sensory branches evenly or whether motor axons are preferentially damaged. It was anticipated that this study would help to define potential targets of future therapies (e.g. axons and/or Schwann cells) and to determine which nerves and morphological parameters should be analysed to evaluate the success of such interventions.

Material and methods

Animals

Homozygous *PMP22*$^{0/0}$ (Agouti SV129EV/C57BL/6) and heterozygous *PMP22*-transgenic (B6C3F1) mice were obtained from our own breeding colonies. Wild-type mice from the same genetic backgrounds were used as controls. The genotypes were assessed by Southern blot analysis of genomic DNA isolated from tail biopsies as described (Adlkofer *et al*., 1995; Magyar *et al*., 1996). Experiments were performed in accordance with the legal requirements of the Eidgenössische Technische Hochschule and Kanton Zürich (Switzerland).

Light and electron microscopy

Ten- to 13-month-old *PMP22*$^{0/0}$ mice, *PMP22*-transgenic mice with additional copies of the *PMP22* gene and wild-type controls were deeply anaesthetized with sodium pentobarbital (100–150 μg/g of body weight) and transcardially perfused with 4% paraformaldehyde and 2% glutaraldehyde in 0.1 M cacodylate buffer pH 7.3. Four to six animals from each group were studied. To be able to compare proximal versus distal levels of the same peripheral nerve, L3 ventral and

dorsal spinal roots (as representatives of the most proximal region of the femoral nerve) and the quadriceps and saphenous nerves (the two main distal branches of the femoral nerve) were dissected. The specimens were post-fixed in the same fixative overnight at 4°C, osmicated and, after dehydration, embedded in Spurr. For morphometrical analysis, 1-μm-thick transverse semithin sections were obtained and stained with alkaline toluidine blue. Special care was taken to obtain sections at the same level from each identical nerve. Ultrathin sections were contrasted with uranyl acetate and lead citrate and examined with a JEOL 100C electron microscope.

Morphometrical analysis

Morphometrical data were collected using the National Institute of Health Image 1.60 software program and a Power Apple-Macintosh 7300/166 computer. A special macro was designed to meet the specific requirements of this type of analysis. Briefly, a 1 μm semithin section of a nerve was visualized in a Zeiss Axiophot microscope with a 630 final magnification, and a series of partially overlapping fields covering the cross-sectional area of the nerve were captured with the help of a KAPPA CCD camera. The overlapping images were transferred to the computer and pasted together to obtain a composite image of the nerve. Next, the nerve was filled up with frames of identical size and nerve fibre profiles within these frames were measured. Frames to be analysed were chosen at random. Depending on the number of myelinated fibres and the size of the nerve, we analysed between 30% and 100% of the fascicular area and, if possible, 200–300 axons per nerve.

The cross-sectional area of the endoneurium, axons and myelinated fibres (fibre = axon plus myelin) were measured for each nerve. To obtain the area of axons and myelinated fibres, a threshold grey-scale level for axons and myelin profiles was defined and used to trace the border of axons and the outer edge of myelin. The diameter of axons and myelinated fibres was mathematically deduced from a circle of an equivalent area. Paranodal regions and Schmidt–Laterman incisures were included in the analysis because these two specific domains of myelinated fibres could not be unequivocally identified in *PMP22*-mutant nerves. Information obtained from control animals showed that the axonal diameter of the smaller myelinated fibres measured at least 1 μm. Therefore, we measured myelinated axons irrespective of their size, and unmyelinated axons with a diameter equal or superior to 1 μm in the L3 ventral roots and quadriceps nerves of the *PMP22*-mutant mice. In the sensory branches of the mutant animals, unmyelinated axons with a diameter between 1 and 1.5 μm could not be quantitatively identified, since the axons were densely packed without enough threshold differences for individualization. Thus, our morphometrical analysis of the sensory branches remained limited to the myelinated fibres.

Quantification and statistical analysis

The following data were obtained and analysed using Microsoft Excel 5 software: number of axons with a diameter $\geqslant$1 μm per nerve; number of myelinated fibres per nerve; distribution of the diameter of axons and myelinated fibres; *g*-ratio (axonal diameter/myelinated fibre diameter) as a function of the axonal diameter. Based on the distribution of the axonal diameters, we classified the axons into three categories according to their diameter: 1–2.99 μm, small; 3–6.99 μm, medium; $\geqslant$7 μm, large. Data were subjected to statistical analysis by the non-parametric Mann–Whitney *U* test using Statview, version 4.0 software. *P* values $\leqslant$ 0.05 were considered to be statistically significant.

Results

To assess quantitatively the degree of myelin and axonal deficiencies due to altered *PMP22* gene dosage, we performed a morphometrical analysis of the roots and peripheral nerves of ~1-year-old *PMP22*$^{0/0}$ mice, transgenic mice carrying additional copies of the *PMP22* gene and age-matched wild-type control animals. We selected aged animals because we reasoned that some changes, like axonal loss, might be more pronounced at advanced stages of the disease. The L3 roots were taken as representatives of the most proximal segment of the PNS, containing axons which are close to the neuronal bodies and are either purely motor (L3 ventral root) or sensory (L3 dorsal root). As the distal counterpart, we chose the quadriceps and saphenous nerves, the two main branches of the femoral nerve. The femoral nerve is the major nerve trunk originating from the lumbar plexus and contains axons from the L3 roots. This analysis also allowed us to obtain information about the deficits in motor branches (ventral roots and quadriceps nerves) compared with sensory branches (dorsal roots and saphenous nerves).

Myelinated fibres

The frequency distribution of the diameter of myelinated fibres of individual control mice showed a bimodal profile for L3 ventral roots and quadriceps nerves, and a unimodal distribution with a predominance of small calibre myelinated fibres for the L3 dorsal roots and saphenous nerves (data not shown). The total number of myelinated fibres in the L3 ventral roots (mean ± SD: 640 ± 118) and quadriceps nerves (557 ± 57) of the wild-type mice was roughly similar, and there was only slight variability between animals. In contrast, the total number of myelinated fibres in the L3 dorsal root (1683 ± 342) was almost double the number of myelinated fibres in the saphenous nerves (838 ± 79). In addition, the number of myelinated fibres in the L3 dorsal root showed the highest variability among individual controls (Fig. 1).

The roots and peripheral nerves of *PMP22*$^{0/0}$ mice displayed a severe reduction of myelinated fibres (Fig. 1) with a more uniform distribution of sizes when compared

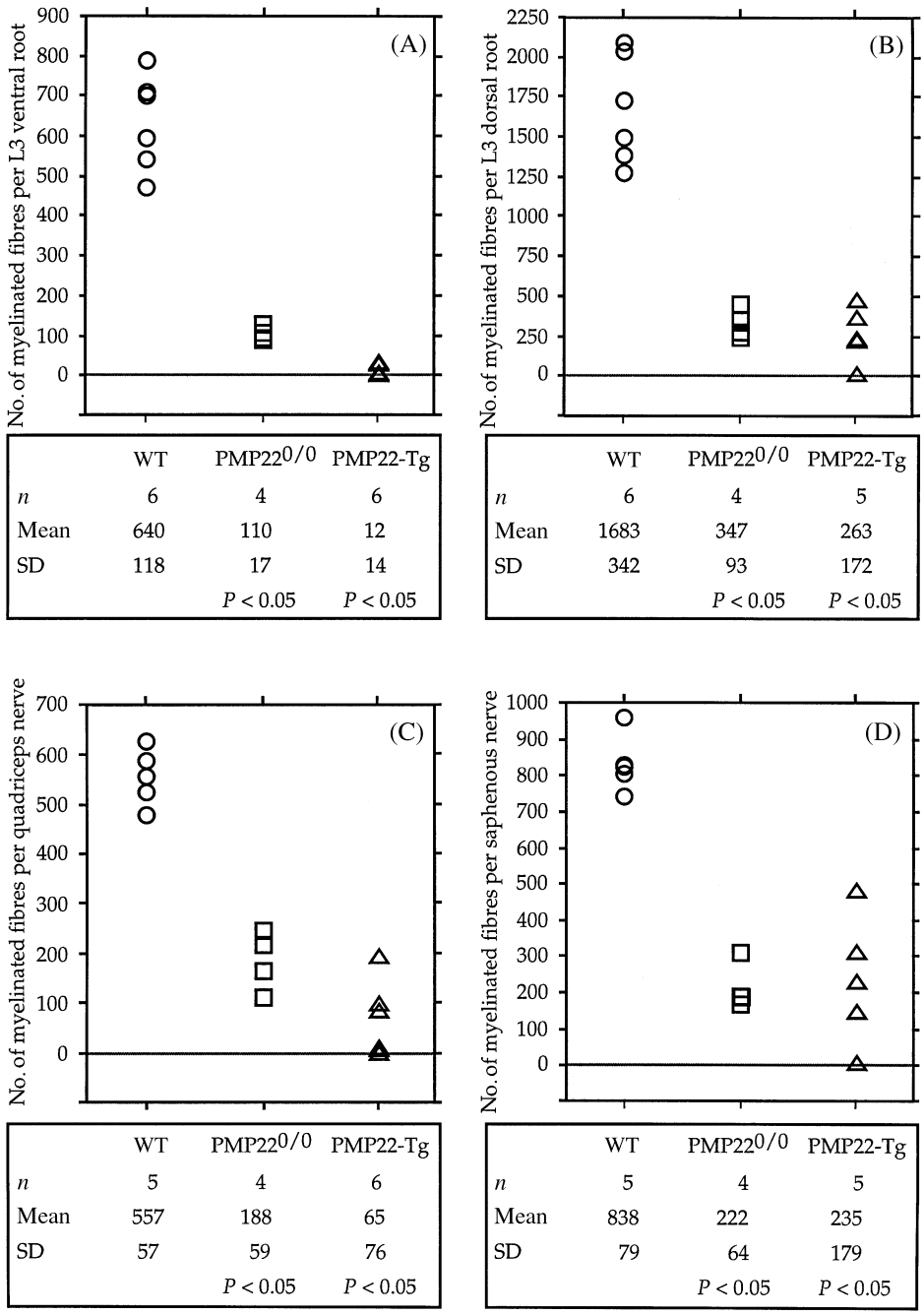

Fig. 1 Number of myelinated fibres per total fascicular area of the L3 ventral (**A**) and dorsal (**B**) roots, quadriceps nerves (**C**) and saphenous nerves (**D**) of control and *PMP22*-mutant mice, as determined using toluidine blue stained transverse semithin sections. A table with a summary of the statistical analysis is shown below each diagram. *P* values were calculated using the non-parametric Mann–Whitney *U* test and reflect comparisons with wild-type (WT) mice.

with controls. All nerve segments showed a unimodal distribution with the main peak usually found between 4 and 7 μm of diameter (data not shown). Myelinated fibres in the L3 ventral roots (110 ± 17) and quadriceps nerves (188 ± 59) were less numerous than in the L3 dorsal roots (347 ± 93) and saphenous nerves (222 ± 64), suggesting that demyelination might affect the motor axons more severely (Fig. 1). To address this issue more closely and because the number of myelinated fibres in control animals was higher in the sensory branches (L3 dorsal roots and saphenous nerves), we calculated the ratio of myelinated fibres between the L3 ventral and dorsal roots (Table 1, VR : DR) and between quadriceps and saphenous nerves (Table 1, QN : SN). The comparison of the values obtained for PMP22$^{0/0}$ mice with wild-type animals showed no statistically significant differences (Table 1). Similar results were obtained when we compared the mean number of myelinated fibres of *PMP22*$^{0/0}$ with wild-type nerves (Table 2).

Table 1 *Ratios of myelinated fibres and myelin-competent axons (mean ± SD)*

	VR : DR myelinated fibres	QN : SN myelinated fibres	QN : VR myelinated fibres	SN : DR myelinated fibres	(QN : VR) axons > 3 μm
Wild-type	0.385 ± 0.062 (n = 6)	0.663 ± 0.091 (n = 4)	0.907 ± 0.123 (n = 5)	0.537 ± 0.099 (n = 5)	0.986 ± 0.102 (n = 5)
PMP22$^{0/0}$	0.335 ± 0.103 (n = 4, ns)	0.873 ± 0.306 (n = 4, ns)	1.731 ± 0.579 (n = 4, $P < 0.05$)	0.645 ± 0.095 (n = 4, ns)	0.393 ± 0.114 (n = 4, $P < 0.05$)
PMP22-Tg	*0.064 ± 0.054* (n = 5, $P < 0.05$)	0.390 ± 0.262 (n = 5, ns)	4.938 ± 6.911 (n = 6, ns)	1.099 ± 0.790 (n = 4, ns)	0.500 ± 0.038 (n = 6, $P < 0.05$)

VR = L3 ventral roots; DR = L3 dorsal roots; QN = quadriceps nerves; SN = saphenous nerves; ns = not significant; Tg = transgenic.

Table 2 *Comparison of myelinated fibres and myelin-competent axons in PMP22-mutant with wild-type mice*

	Myelinated fibres				Axons >3 μm	
	VR	QN	DR	SN	VR	QN
PMP22$^{0/0}$ (%)	17	34	20	26	89	35
PMP22-Tg (%)	2	12	16	28	96	51

Percentages were calculated between the mean values for PMP22-mutant nerves and the mean values for wild-type nerves. VR = L3 ventral roots; QN = quadriceps nerves; DR = L3 dorsal roots; SN = saphenous nerves.

Since the loss of myelinated fibres in the saphenous nerves of CMT1 patients appears to be more severe at distal levels (Dyck *et al.,* 1993), we wanted to determine whether a similar finding can be observed in *PMP22*$^{0/0}$ mice. In contrast, the reduction of myelinated fibres in *PMP22*$^{0/0}$ L3 ventral roots (17% of controls) was more severe than in PMP22$^{0/0}$ quadriceps nerves (34% of control; Table 2). Similarly, the high ratio of myelinated fibres between the quadriceps nerves and the L3 ventral roots of *PMP22*$^{0/0}$ mice (Table 1, QN : VR) indicates that demyelination was more advanced in the roots than in the peripheral nerves. A similar tendency was observed for the sensory branches (Table 1, SN : DR, and Table 2), but the slightly higher ratios obtained for the *PMP22*$^{0/0}$ nerves do not statistically differ from the corresponding wild-type values.

PMP22-transgenic mice were quite variable concerning the number of myelinated fibres present in their nerves except for the L3 ventral roots which were almost completely amyelinated in all animals (Fig. 1 and Table 2). The quadriceps nerve was the second most affected nerve with three out of six mice having none or only few myelinated fibres (Fig. 1 and Table 2). Four out of five *PMP22*-transgenic mice had a significant number of myelinated fibres in the L3 dorsal roots and saphenous nerves preserved, whereas a fifth mouse had only very few myelinated fibres (Fig. 1). The ratios of myelinated fibres between the peripheral nerves and roots further illustrates the high variability of myelination present in the *PMP22*-transgenic nerves (Table 1). As a result of this variability, only the ratios between the L3 ventral and dorsal roots were statistically significant reflecting the fact that sensory axons were significantly myelinated in some *PMP22*-transgenic mice (Table 1).

g-Ratios

The scatter diagram of the *g*-ratio against axon diameter correlates changes of myelin thickness in relation to axonal size (Fig. 2). In control nerves, most axons had *g*-ratios between 0.6 and 0.8. Values below 0.6 were usually due to the presence of Schmidt–Laterman incisures and paranodal regions. The nerves of *PMP22*$^{0/0}$ mice had an increased scatter of *g*-ratios with many unusually low values. Very low *g*-ratios were invariably associated with small calibre,

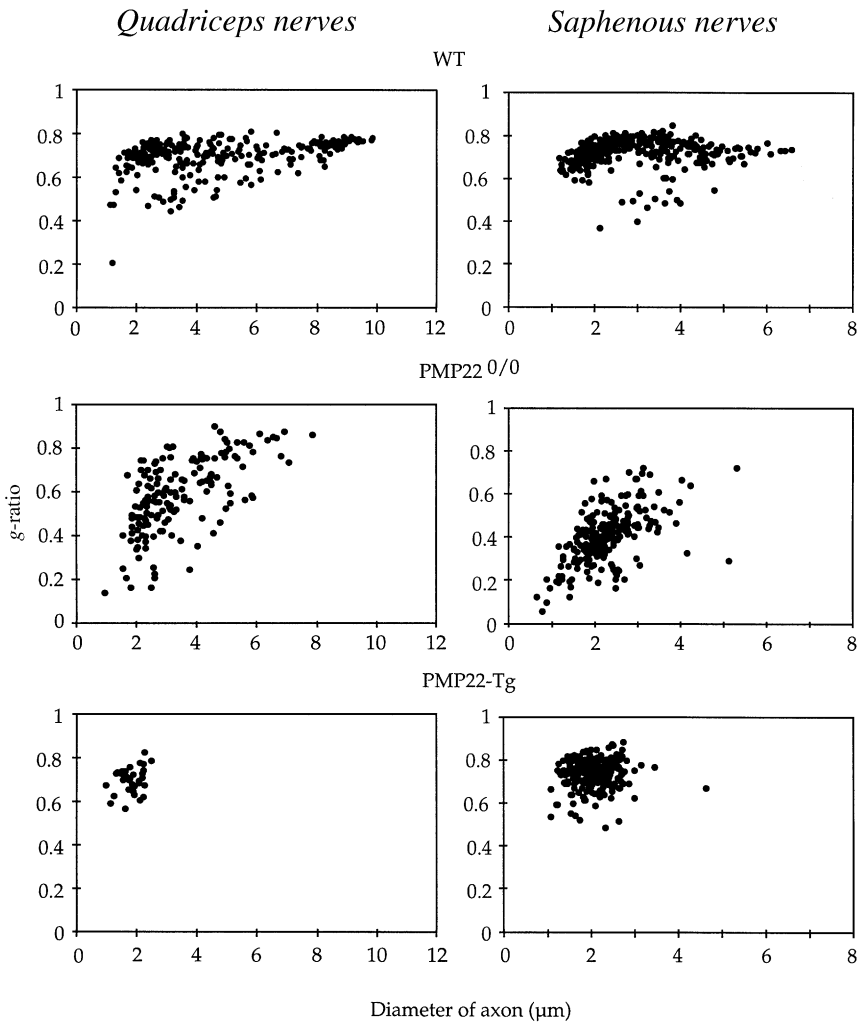

Fig. 2 Scatter diagrams of *g*-ratios as function of axon diameters of the quadriceps nerve (*left panel*) and saphenous nerve (*right panel*) of representative wild-type (WT) and *PMP22*-mutant mice. Fibres with low *g*-ratio values in WT nerves reflect uncompact myelin regions (Schmidt–Laterman incisures and paranodal regions). The increased dispersion of *g*-ratios in *PMP22*$^{0/0}$ nerves are due to the presence of tomacula and remyelinated fibres.

Table 3 *Percentage of* g*-ratio values >0.8 in* PMP22$^{0/0}$ *nerves (mean ± SD)*

VR	DR	QN	SN
20 ± 12	1.6 ± 1.2	12 ± 3	0.17 ± 0.34

n = 4; VR = L3 ventral roots; DR = L3 dorsal roots; QN = quadriceps nerves; SN = saphenous nerves.

probably atrophic axons. Only few large calibre axons were myelinated. They usually had high *g*-ratios suggesting remyelinated axons because congenital hypomyelination is not a feature of *PMP22*$^{0/0}$ nerves during post-natal development (Adlkofer *et al.,* 1995). Axons with high *g*-ratios were more frequent in the motor branches than in sensory nerves (Fig. 2 and Table 3).

In *PMP22*-transgenic mice whose nerves contained myelinated fibres, the *g*-ratio distribution revealed that mainly the small calibre axons were myelinated. Axons either had a myelin sheath of appropriate thickness or were hypomyelinated (Fig. 2).

Axonal deficiency

Since the nerves of the examined *PMP22*-mutant animals contain many large non-myelinated axons in a 1 : 1 relationship with their Schwann cells (which are normally myelinating), we estimated the diameter size and distribution of myelin-competent axons. This analysis was designed to give an indication of the fate of such an axonal population, regardless of their myelination status. The examination of the axonal diameter of myelinated fibres from control nerves showed that over 99.8% of myelinated axons have a diameter ⩾1 μm. Thus, we included all axons with a diameter of 1 μm or above as part of the myelin-competent axonal population in the analysis of *PMP22*-mutant nerves.

The frequency distribution of the diameter of myelinated

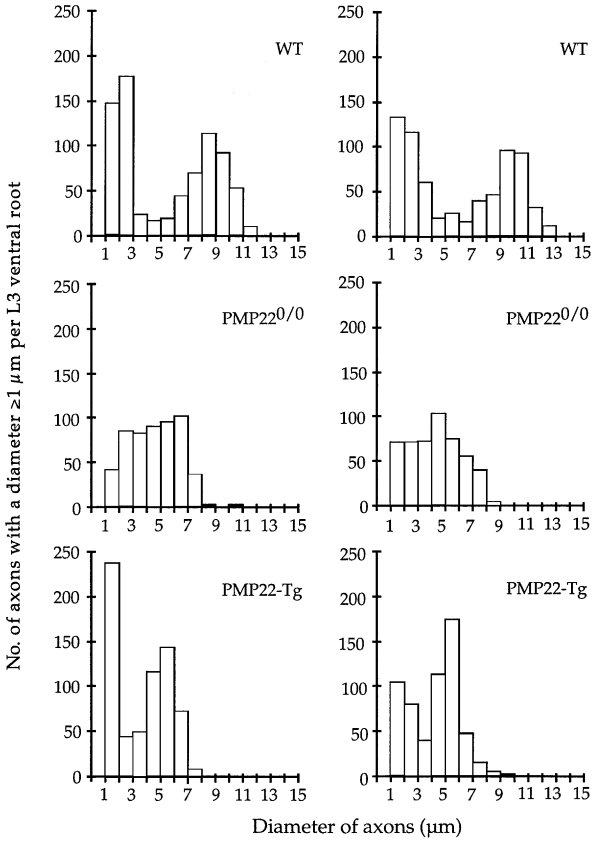

L3 Ventral roots

	Diameter 1-3 μm	Diameter 3-7 μm	Diameter ≥ 7 μm
	Mean ± SD	Mean ± SD	Mean ± SD
Wild-type	248 ± 52	113 ± 17	279 ± 62
$n = 6$			
PMP22$^{0/0}$	131 ± 18	317 ± 48	34 ± 14
$n = 4$	$P < 0.05$	$P < 0.05$	$P < 0.05$
PMP22-Tg	225 ± 64	338 ± 57	38 ± 30
$n = 6$	n.s.	$P < 0.05$	$P < 0.05$

Fig. 3 Histograms showing the distribution of axons with a diameter ⩾1 μm in the L3 ventral roots of two representative mice from each group (wild-type, WT; *PMP22*$^{0/0}$ and *PMP22*-transgenic mice). Next to the histograms a summary of the statistical analysis is given. For this analysis, axons were divided in three categories: small (1–3 μm), medium (3–7 μm) and large (⩾7 μm). *P* values were calculated using the non-parametric Mann–Whitney *U* test (comparisons with WT mice). n.s. = not significant; Tg = transgenic.

axons from control L3 ventral roots showed a bimodal distribution with a first peak between 1 and 3 μm and a second peak between 7 and 11 μm (Fig. 3). This bimodal distribution was usually lost in the L3 ventral roots of *PMP22*$^{0/0}$ or transgenic mice. Axons with a diameter >7 μm were scarce in both PMP22-mutants, although an increase of the population of medium size axons (between 3 and 7 μm) was apparent (Fig. 3). In addition, the number of small calibre axons (between 1 and 3 μm) was also reduced in *PMP22*$^{0/0}$ mice. Moreover, the total number of axons of a diameter ⩾1 μm in the L3 ventral roots of two *PMP22*$^{0/0}$ mice was slightly decreased compared with controls and *PMP22*-transgenic mice (Fig. 4).

The frequency distribution of the diameter of myelinated axons from the quadriceps nerves of wild-type mice showed a peak at the low calibre range (2–3 μm), whereas the medium and large calibre axons were more uniformly distributed. The quadriceps nerves of *PMP22*$^{0/0}$ and transgenic mice showed a severe reduction of axons with a diameter >7 μm and a significant decrease of axons of medium size (between 3 and 7 μm; Fig. 5). Furthermore, the total number of axons with a diameter ⩾1 μm in the quadriceps of both mutant mice was reduced compared with controls (Fig. 4). This reduction was more pronounced in *PMP22*$^{0/0}$ mice than in *PMP22*-transgenic animals. To evaluate whether the reduced number of axons was more severe in distal segments, we determined the ratio of axons with a diameter ⩾1 μm between the quadriceps nerves and L3 ventral roots. The ratios of both groups of *PMP22*-mutant mice compared with the ratios of wild-type animals did not reach statistical significance (data not shown). However, when only the middle and large size axonal populations (>3 μm) were considered, axon deficiency was much more severe in the quadriceps nerves of both strains of *PMP22*-mutant mice (Table 1, QN : VR, and Table 2).

Electron microscopy

The morphometrical data indicated a pronounced reduction of large calibre axons in the nerves of the *PMP22*-mutant mice. To evaluate whether axonal degeneration contributes to this observation, we analysed the ultrastructure of the L3 spinal roots and peripheral nerves of two *PMP22*$^{0/0}$ and two *PMP22*-transgenic mice in comparison with control animals.

The L3 roots and peripheral nerves of both types of *PMP22*-mutant mice showed an obvious deficiency of large calibre axons when compared with wild-type controls (Fig. 6). In the L3 ventral roots and quadriceps nerves of *PMP22*-

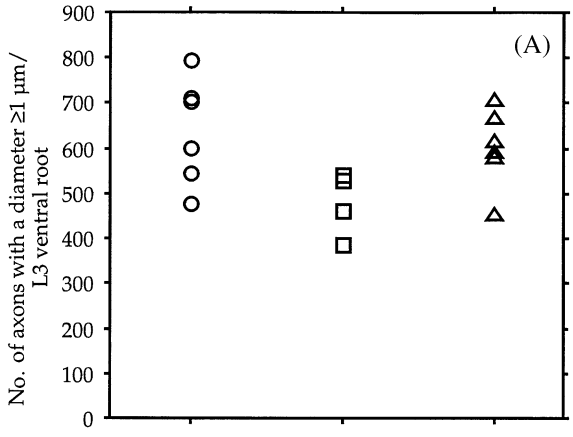

	WT	PMP22 $^{0/0}$	PMP22-Tg
n	6	4	6
Mean	640	482	601
SD	118	71	88
		$P < 0.05$	n.s.

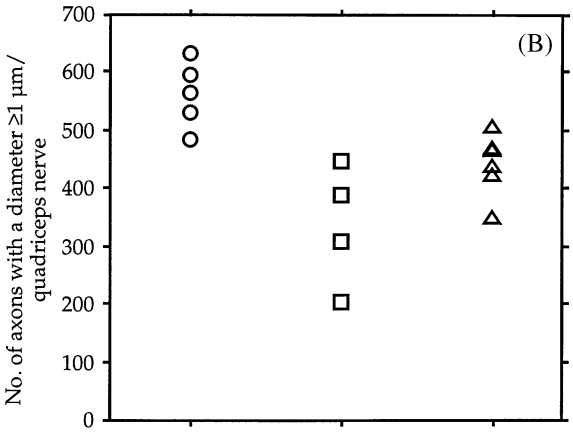

	WT	PMP22 $^{0/0}$	PMP22-Tg
n	5	4	6
Mean	557	333	436
SD	57	105	54
		$P < 0.05$	$P < 0.05$

Fig. 4 Number of axons with a diameter ⩾1 µm per total fascicular area of the L3 ventral roots (**A**) and quadriceps nerves (**B**) of control and *PMP22*-mutant mice as analysed using toluidine blue-stained transverse semithin sections. Below each diagram, a summary of the statistical analysis is shown. *P* values were calculated using the non-parametric Mann–Whitney *U* test (comparisons with wild-type, WT, mice). n.s. = not significant; Tg = transgenic.

transgenic mice, large and medium size axons were amyelinated and only very few small myelinated fibres were seen (Fig. 6E). In contrast, the L3 dorsal roots and saphenous nerves contained some myelinated fibres (Fig. 6F) which had either a myelin sheath of normal thickness or were thinly myelinated. Some axons were only surrounded by a few wraps of myelin and in some, the myelin sheaths appeared not fully compacted. Occasionally, myelin debris was found in macrophages or Schwann cells. Schwann cell onion bulb formation was not a prominent feature in the nerves of the *PMP22*-transgenic mice although remains of basal laminae were often seen around axons. Evident signs of axonal damage were not observed.

Most large calibre axons were not myelinated in the L3 ventral roots and quadriceps nerves of *PMP22*$^{0/0}$ mice (Fig. 6C). Few of them, however, were associated with a thin myelin sheath. Hypermyelination with formation of redundant myelin loops, most probably reflecting tomacula, was a common feature in all nerves of *PMP22*$^{0/0}$ mice (Adlkofer *et al.,* 1995), but this pathology was more frequent in the L3 dorsal roots and saphenous nerves (Fig. 6D). Tomacula usually displaced and compressed the associated axons. Most axons in peripheral nerves and L3 roots were surrounded by onion bulbs consisting of slender cytoplasmic Schwann cell processes and basal lamina. However, these onion bulbs were not as well developed as in human CMT1 nerves (Thomas *et al.*, 1997).

Indicative changes of axonal damage were found only in the nerves of *PMP22*$^{0/0}$ mice. Structural abnormalities were characterized by an accumulation of dense bodies and vesicles, vacuolization of axonal organelles, disruption of the axolemma and disorganization of cytoskeletal elements (Fig. 7A–C). In the saphenous nerves, Schwann cells surrounding myelin debris without any axonal profile in their cytoplasm were frequently observed, suggesting that the axon had degenerated (Fig. 7D). Occasionally, Schwann cell lamellae of onion bulbs contained a small non-myelinated axon, most probably representing axonal sprouting. Although some of these morphological changes observed in *PMP22*$^{0/0}$ nerves might be age-related, the results are consistent with the morphometric analysis indicating pronounced axonal deficits in these mouse mutants.

Discussion

Despite the qualitative differences in myelination that characterize *PMP22*$^{0/0}$ and *PMP22*-transgenic mice, both mouse strains display a similar spatial distribution of myelin abnormalities. Quantitative analysis of myelinated fibres in the L3 roots and the quadriceps and saphenous nerves of both *PMP22*-mutant animals revealed that myelin deficits affect the ventral roots more severely than peripheral nerves. While the ratios between motor and sensory nerves in *PMP22*$^{0/0}$ mice showed similar preservation of myelinated fibres, *g*-ratios indicated that the demyelination process is more advanced in the motor branches. Similarly, sensory branches of some *PMP22*-transgenic mice contained a significant number of myelinated small calibre axons. Somatic transgene inactivation was suggested as a plausible hypothesis to account for the presence of a few thinly myelinated axons in the nerves of young *PMP22*-transgenic mice (Magyar

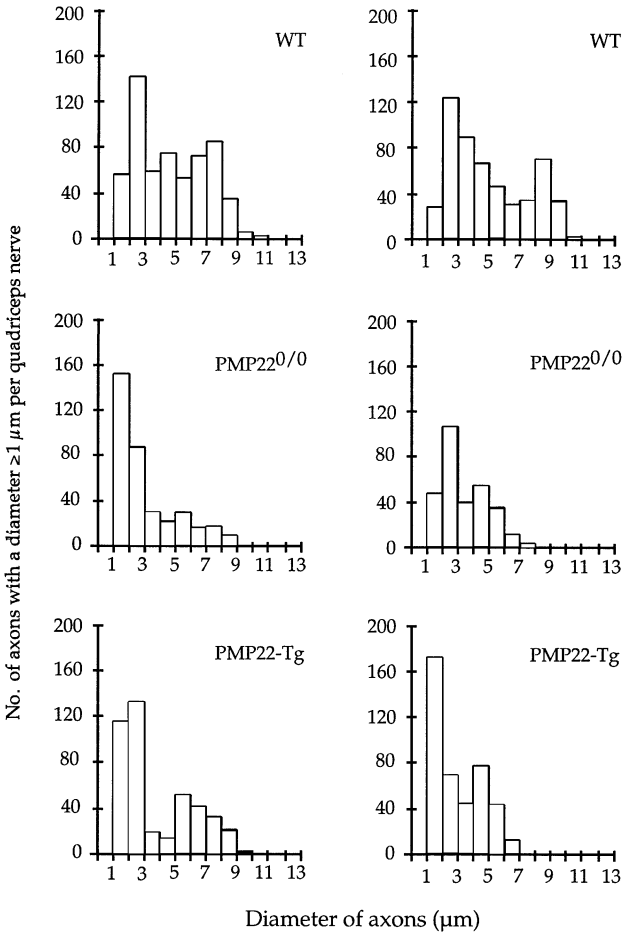

Quadriceps nerves

	Diameter 1-3 μm	Diameter 3-7 μm	Diameter ≥ 7 μm
	Mean ± SD	Mean ± SD	Mean ± SD
Wild-type	188 ± 28	240 ± 33	129 ± 13
$n = 5$			
PMP22$^{0/0}$	198 ± 81	125 ± 31	6 ± 4
$n = 4$	n.s.	$P < 0.05$	$P < 0.05$
PMP22-Tg	249 ± 52	120 ± 27	67 ± 41
$n = 6$	$P < 0.05$	$P < 0.05$	$P < 0.05$

Fig. 5 Histograms demonstrating the distribution of axons with a diameter ⩾1 μm in the quadriceps nerves of two representative mice from each group (wild-type, WT; *PMP22*$^{0/0}$ and *PMP22*-transgenic mice). Next to the histograms, a summary of the statistical analysis is shown for each group of mice. For this analysis axons were divided in three categories: small (1–3 μm), medium (3–7 μm) and large (⩾7 μm). *P* values were calculated using the non-parametric Mann–Whitney *U* test (comparisons with WT mice). n.s. = not significant; Tg = transgenic.

et al., 1996). Considering the number of myelinated fibres present in old *PMP22*-transgenic nerves, such a mechanism seems unlikely unless Schwann cells which have inactivated the transgene have a proliferation or survival advantage. Alternatively, Schwann cells associated with small calibre sensory axons might be less vulnerable to *PMP22* gene dosage.

The predilection of myelin defects for motor nerves has previously been noticed in *PMP22*-mutant animals (Adlkofer *et al*., 1995; Sereda *et al*., 1996), heterozygous protein zero (P_0) knockout mice (Martini *et al*., 1995; Shy *et al*., 1997), and connexin 32 (Cx32) knockout mice (Anzini *et al*., 1997; Scherer *et al*., 1998). Such a distribution is intriguing for a genetic defect which should affect myelinating Schwann cells evenly. Since the available evidence supports a common developmental origin for all types of Schwann cells found in mature peripheral nerves, other factors, such as specific axon–glia interactions, might be responsible for this peculiar distribution. With the exception of neurons responsible for proprioception, motor neurons have larger calibre axons than sensory neurons and, as a consequence, motor nerves contain a higher percentage of large fibres. Consistently, most myelinated axons in *PMP22*-mutant nerves were of small calibre. Furthermore, ventral roots which only contain the axons of motor neurons display the most severe myelination defect in both *PMP22*-mutant strains. Thus, our data support the hypothesis that Schwann cells myelinating large caliber axons, such as motor neurons and proprioception sensory neurons, might be more vulnerable to myelin gene defects. However, the increased susceptibility of large axons to abnormal myelination might also be partially attributed to PMP22 expression by motor neurons (Parmantier *et al*., 1995). Furthermore, the possibility that the thicker myelin sheath of large axons is more susceptible to disturbances of myelin stability remains open.

Morphometrical analysis of axonal calibre demonstrated a striking deficit of large axons with a diameter superior to 7 μm in the motor branches (L3 ventral roots and quadriceps nerves) of both *PMP22*$^{0/0}$ and transgenic mice. This axonal deficiency might be explained by reduced axonal calibre

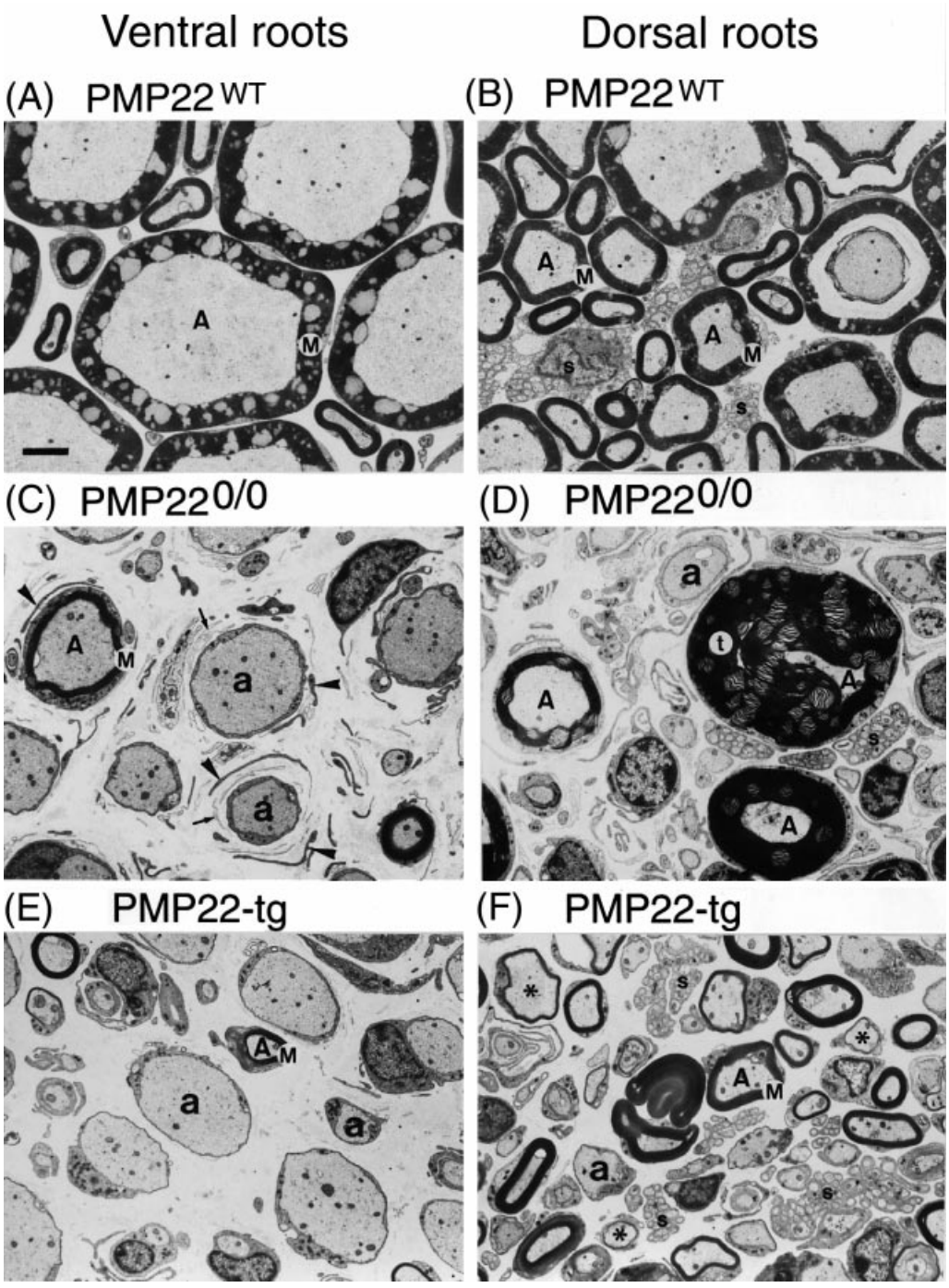

Fig. 6 Electron micrographs comparing the ultrastructure of the L3 ventral roots (**A**, **C**, **E**) and L3 dorsal roots (**B**, **D** and **F**) of wild-type (**A** and **B**), *PMP22*$^{0/0}$ (**C** and **D**) and *PMP22*-transgenic (**E** and **F**) mice. (**A** and **B**) Wild-type roots showing normally myelinated fibres (A). Several non-myelinating Schwann cells are seen in the dorsal root in association with small calibre axons (s). Comparison between the ventral (**C**) and dorsal (**D**) root of a *PMP22*$^{0/0}$ mouse: in the ventral root many axons are demyelinated (a) and only few myelinated fibres are present (A). Myelinated fibres are more abundant in the dorsal root, where hypermyelination and tomacula (t) are seen. Onion bulbs consisting of thin Schwann cells cytoplasmic lamellae (arrowheads) and basal lamina (arrows) are present around many axons. Comparison between the ventral (**E**) and the dorsal (**F**) root of a *PMP22*-transgenic mouse, showing many amyelinated axons (a) in the ventral root and abundant myelinated fibres (A), some of them thinly myelinated (asterisks), in the dorsal root. Note the increased cytoskeletal density of the axoplasma and the absence of large calibre axons in the roots of *PMP22*-mutant mice. M = compact myelin; Tg = transgenic. Bar = 3 μm.

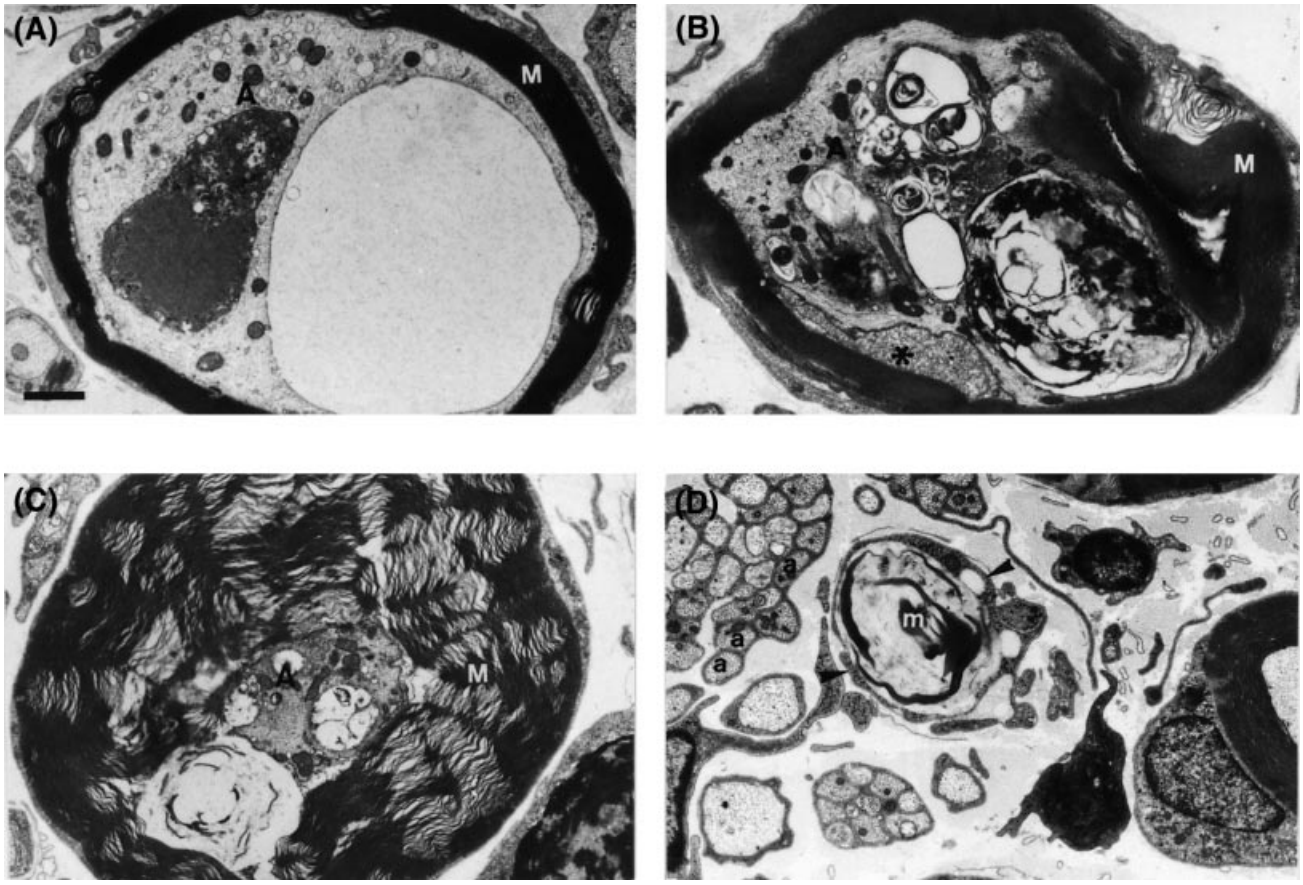

Fig. 7 Ultrastructure of selected abnormal axons in the nerves of *PMP22*$^{0/0}$ mice. Transverse sections from the L3 ventral root (**A**) and saphenous nerve (**B**–**D**). (**A**) The axoplasm (A) of this myelinated fibre contains a large vacuole filled with granular and filamentous material and a dense osmophilic body of complex structure, besides many membrane-bound vesicles. (**B**) Myelinated fibre with partially folded, degenerating myelin. The axoplasm (A) is highly distorted by multiple inclusion bodies and disorganized neurofilaments. The adaxonal Schwann cell cytoplasm (asterisk) has a granular appearance. (**C**) Hypermyelinated fibre with a small, very dense axon (A) containing several membrane-bound vacuoles and mitochondria. (**D**) Schwann cell cytoplasmic processes (arrowheads) devoid of discernible associated axon profiles surround a membranous myelin-like debris (m). M = compact myelin; a = unmyelinated axons. Bar = 1 μm.

because a shift of axonal diameter to a smaller size with a concomitant relative increase of medium or small calibre axons was observed. Most hypermyelinated axons in the *PMP22*$^{0/0}$ mice were of small diameter, suggesting a direct relationship between hypermyelination and reduced axonal calibre. However, the mechanisms leading to the observed pathology are likely to be multifactorial. During development of the PNS, axons attain their final calibre progressively in two well-defined phases. After axons have contacted their targets and synapses are formed, axonal growth best correlates with the amount of microtubules. A further increase of axonal calibre, known as radial growth, is tightly coupled with myelination and is associated with increased neurofilament (NF) content (reviewed by Hoffman and Griffin, 1993). If myelination is necessary for normal radial growth during axonal maturation, defective radial growth might be expected to occur in *PMP22*-transgenic mice since their nerves remain largely amyelinated (Magyar *et al*., 1996). Similarly, *PMP22*$^{0/0}$ mice have a dysmyelinating phenotype with highly perturbed myelination. Thus, radial growth may also be altered in these animals. Although myelination *per se* is not required for the radial growth of axons in the optic nerve (Sanchez *et al*., 1996), the situation may differ in the PNS. Large calibre axons do not develop in the peripheral nerves of the *Tr* mouse suggesting that a competent myelinating Schwann cell is required for normal radial growth in the PNS (Ayers and Anderson, 1976). An alternative or additional mechanism to account for the reduced axonal calibre present in *PMP22*-mutant mice is axonal atrophy which could develop or increase over time. Such a process is likely to be responsible for the reduction of axonal calibre observed in MAG (myelin-associated glyocoprotein) knockout mice. Axonal radial growth proceeds normally in these mutant mice but they exhibit a reduction of the mean diameter of myelinated axons when adult (Yin *et al*., 1998).

NF number and NF spacing are two important intrinsic factors that determine axon calibre (reviewed by Hoffman and Griffin, 1993; Xu *et al*., 1996; Zhu *et al*., 1997; Elder *et al*., 1998). A progressive increase of NF synthesis together with a concomitant decline of NF transport modulates NF

number during the radial growth of developing axons, and similar changes occur during regeneration of peripheral axons (reviewed by Hoffman and Griffin, 1993). In addition, alterations in NF spacing contribute to local variations of calibre along axons (Hsieh *et al.,* 1994). Most probably myelinating Schwann cells locally regulate NF spacing by modulating the phosphorylation of NF-H and NF-M subunits (de Waegh *et al.*, 1992). It is conceivable that any of these factors, alone or in combination, may be responsible for the reduced axonal calibre observed in *PMP22*-mutant mice. Indeed, reduced axonal caliber in the dysmyelinated nerves of *Tr* mice correlate with increased density of axonal cytoskeletal elements (Low, 1976), reduced NF spacing and reduced NF phosphorylation (de Waegh and Brady, 1991; deWaegh *et al.*, 1992). Similarly, the reduction of axon calibre in MAG knockout mice is associated with a decrease of NF spacing and reduced phosphorylation of the NF-high molecular weight and NF-medium molecular weight subunits (Yin *et al*., 1998). Although we did not quantify NF density in our mutants, axonal cytoskeleton appeared more closely packed in *PMP22*-mutant nerves compared with controls.

In our study, the population of myelin-competent axons was decreased in the L3 ventral roots and quadriceps nerves of *PMP22*$^{0/0}$ mice and, to a lesser extent, in the quadriceps nerves of *PMP22*-transgenic mice suggesting that additional factors besides decreased axonal caliber might contribute to axonal loss. Additionally, morphological evidence for axonal damage and degeneration was found in the nerves of *PMP22*$^{0/0}$ mice. Axonal degeneration is being recognized as a quite common finding in both the PNS (Giese *et al*., 1992; Fruttiger *et al*., 1995; Anzini *et al*., 1997; Yin *et al*., 1998) and CNS (Anderson *et al*., 1998; Griffiths *et al*., 1998) of mice with mutations in myelin genes, but the responsible cellular and molecular mechanisms are largely unknown. The presence of axonal spheroids in the CNS of proteolipid protein (PLP) knockout and transgenic mice hints at altered axonal transport as a possible cause of fibre degeneration in these animals (Anderson *et al*., 1998; Griffiths *et al.*, 1998). Axonal atrophy was considered to predispose to axonal degeneration in P_0 and MAG knockout mice (Giese *et al.,* 1992; Yin et *al.*, 1998). However, decreased axonal calibre *per se* may not be sufficient to cause axonal degeneration because mice with targeted null mutations for NF-L and NF-M subunits behave normally and do not show signs of axonal degeneration despite a severe impairment of axonal radial growth (Zhu *et al*., 1997; Elder *et al*., 1998). Chronic deprivation of neurotrophic factors might also contribute to axonal degeneration since myelinating Schwann cells express a different repertoire of neurotrophic factors compared with non-myelinating Schwann cells (Friedman *et al*., 1996). Interestingly, we could not identify morphological signs of degeneration in the amyelinated axons of *PMP22*-transgenic mice, whereas degenerating axons in *PMP22*$^{0/0}$ mice were always associated with a myelin sheath. These findings may suggest that axonal degeneration is triggered by factors associated with myelinating Schwann cells, but it cannot be excluded that amyelinated/demyelinated axons indeed degenerate, but morphological changes of degeneration remained unrecognized (Anderson *et al.*, 1998).

Similarly to CMT1 disease in humans (Dyck *et al.*, 1993), *PMP22*$^{0/0}$ and transgenic mice develop a distally related axonopathy since the reduction of medium and large calibre axons is more severe in the quadriceps nerves than in the L3 ventral roots. Axons depend on the neuronal body for the supply of some vital organelles, such as mitochondria, and also newly synthesized proteins must be transported to their final destination for local assembly or secretion. Thus, it appears likely, that neurons with large and long axons have higher demands to maintain the integrity of their peripheral processes and they are probably more sensitive to factors perturbing their function. It is also to be expected that long axons would be more vulnerable than short axons if axonal transport is impaired. There is evidence that Schwann cells strategically positioned along the axon might help to regulate the transport or delivery of proteins to their specific localization along the axon. Myelinated axons show local variation of NF number with more NF in the internode than in the node of Ranvier (Hsieh *et al*., 1994). Furthermore, hypomyelinated *Tr* nerves have a slower rate of transport of NF subunits as well as a fraction of tubulins, and graft experiments suggest that Schwann cells locally modulate slow axonal transport (deWaegh and Brady, 1990; deWaegh *et al.*, 1992).

Although CMT1 is primarily regarded as a demyelinating neuropathy, a long-standing point of view has been entertained that a distal axonopathy may contribute to the clinical progression of the disease. In particular, the distribution of muscle weakness and atrophy, and the pattern of sensory loss in CMT1 patients implies that distal nerves are more vulnerable. Additional evidence for this distal involvement came from the analysis of various levels of CMT1 saphenous nerves. The study showed that the frequency of demyelination and remyelination was higher in the distal segment compared with more proximal segments. Moreover, the quantification of myelinated fibres clearly indicated that loss of myelinated fibres was more severe distally and these data have been interpreted as a sign of axonal atrophy (Dyck *et al.,* 1993). Reduced axonal size in CMT1 nerves has been shown to correlated with decreased NF number (Nukada and Dyck, 1984), hypophosphorylation of NF subunits and abnormal isoform composition of *b*-tubulin (Watson *et al.,* 1994). Moreover, myelin deficits are already present very early in CMT1 patients (Gabreels-Festen *et al.,* 1995) and nerve conduction velocity remains quite stable during the course of the disease (Dyck *et al*., 1989). Thus, axonopathy is a likely explanation for the progressive muscle atrophy and clinical deficits in CMT1 patients. It remains to be determined, however, whether muscle weakness and wasting is more severe distally in *PMP22*$^{0/0}$ and transgenic mice.

In conclusion, a strong agreement exists between the data obtained from CMT1 nerves and animal models for CMT1 disease, and the combined evidence indicates that axonal

involvement is a crucial pathogenic factor. The distally accentuated axonopathy probably develops gradually and contributes to the disease progression. It remains a challenge for future research to elucidate the molecular basis of the abnormal Schwann cell–axon interactions leading to axonal pathology. *PMP22*-mutant mice and other animal models of CMT1, such as P_0 and Cx32 knockout mice, will be invaluable tools to achieve this goal.

Acknowledgements

We wish to thank C. El-Ariss for excellent technical assistance and Dr W. Stahel for expert statistical advice. This work was supported by the Swiss National Science Foundation and the NFP38 program on Research on Neurodegenerative Disease (NFP38).

References

Adlkofer K, Martini R, Aguzzi A, Zielasek J, Toyka KV, Suter U. Hypermyelination and demyelinating peripheral neuropathy in Pmp22-deficient mice. Nat Genet 1995; 11: 274–80.

Adlkofer K, Frei R, Neuberg DH, Zielasek J, Toyka KV, Suter U. Heterozygous peripheral myelin protein 22-deficient mice are affected by a progressive demyelinating tomaculous neuropathy. J Neurosci 1997; 17: 4662–71.

Anderson TJ, Schneider A, Barrie JA, Klugmann M, McCulloch MC, Kirkham D, et al. Late-onset neurodegeneration in mice with increased dosage of the proteolipid protein gene. J Comp Neurol 1998; 394: 506–19.

Anzini P, Neuberg DH-H, Schachner M, Nelles E, Willecke K, Zielasek J, et al. Structural abnormalities and deficient maintenance of peripheral nerve myelin in mice lacking the gap junction protein connexin 32. J Neurosci 1997; 17: 4545–51

Ayers MM, Anderson RM. Development of onion bulb neuropathy in the Trembler mouse. Morphometric study. Acta Neuropathol (Berl) 1976; 36: 137–52.

Birouk N, Gouider R, Le Guern E, Gugenheim M, Tardieu S, Maisonobe T, et al. Charcot–Marie–Tooth disease type 1A with 17p11.2 duplication. Clinical and electrophysiological phenotype study and factors influencing disease severity in 119 cases. Brain 1997; 120: 813–23.

Bort S, Nelis E, Timmerman V, Sevilla T, Cruz-Martinez A, Martinez F, et al. Mutational analysis of the MPZ, PMP22 and Cx32 genes in patients of Spanish ancestry with Charcot-Marie-Tooth disease and hereditary neuropathy with liability to pressure palsies. Hum Genet 1997; 99: 746–54.

Chance PF, Alderson MK, Leppig KA, Lensch MW, Matsunami N, Smith B, et al. DNA deletion associated with hereditary neuropathy with liability to pressure palsies. Cell 1993; 72: 143–51.

De Jonghe P, Timmerman V, Nelis E, Martin J-J, Van Broeckhoven C. Charcot-Marie-Tooth disease and related peripheral neuropathies. J Periph Nerv System 1997; 2: 370–87.

de Waegh S, Brady ST. Altered slow axonal transport and regeneration in a myelin-deficient mutant mouse: the trembler as an in vivo model for Schwann cell-axon interactions. J Neurosci 1990; 10: 1855–65.

de Waegh SM, Brady ST. Local control of axonal properties by Schwann cells: neurofilaments and axonal transport in homologous and heterologous nerve grafts. J Neurosci Res 1991; 30: 201–12.

de Waegh SM, Lee VM, Brady ST. Local modulation of neurofilament phosphorylation, axonal caliber, and slow axonal transport by myelinating Schwann cells. Cell 1992; 68: 451–63.

Dyck PJ, Lambert EH. Lower motor and primary sensory neuron diseases with peroneal muscular atrophy. I. Neurologic, genetic and electrophysiological findings in hereditary polyneuropathies. Arch Neurol 1968a; 18: 603–18.

Dyck PJ, Lambert EH. Lower motor and primary sensory neuron diseases with peroneal muscular atrophy. II. Neurologic, genetic and electrophysiologic findings in various neuronal degenerations. Arch Neurol 1968b; 18: 619–25.

Dyck PJ, Karnes JL, Lambert EH. Longitudinal study of neuropathic deficits and nerve conduction abnormalities in hereditary motor and sensory neuropathy type 1. Neurology 1989; 39: 1302–8.

Dyck PJ, Chance P, Lebo R, Carney JA. Hereditary motor and sensory neuropathies. In: Dyck PJ, Thomas PK, Griffin JW, Low PA, Podulso JF, editors. Peripheral neuropathy. 3rd ed. Philadelphia: W.B. Saunders; 1993. p. 1094–136.

Elder GA, Friedrich VL Jr, Bosco P, Kang C, Gourov A, Tu P-H, et al. Absence of the mid-size neurofilament subunit decreases axonal calibers, levels of light neurofilament (NF-L), and neurofilament content. J Cell Biol 1998; 141: 727–39.

Friedman HC, Jelsma TN, Bray GM, Aguayo AJ. A distinct pattern of trophic factor expression in myelin-deficient nerves of Trembler mice: implications for trophic support by Schwann cells. J Neurosci 1996; 16: 5344–50.

Fruttiger M, Montag D, Schachner M, Martini R. Crucial role for the myelin-associated glycoprotein in the maintenance of axon-myelin integrity. Eur J Neurosci 1995; 7: 511–5.

Gabreels-Festen AA, Bolhuis PA, Hoogendijk JE, Valentijn LJ, Eshuis EJ, Gabreels FJ. Charcot-Marie-Tooth disease type 1A: morphological phenotype of the 17p duplication versus PMP22 point mutations. Acta Neuropathol (Berl) 1995; 90: 645–9.

Giese KP, Martini R, Lemke G, Soriano P, Schachner M. Mouse P0 gene disruption leads to hypomyelination, abnormal expression of recognition molecules, and degeneration of myelin and axons. Cell 1992; 71: 565–76.

Griffiths I, Klugmann M, Anderson T, Yool D, Thomson C, Schwab MH, et al. Axonal swellings and degeneration in mice lacking the major proteolipid of myelin. Science 1998; 280: 1610–3.

Harding AE. From the syndrome of Charcot, Marie and Tooth to disorders of peripheral myelin proteins. [Review]. Brain 1995; 118: 809–18.

Hoffman PN, Griffin JW. The control of axonal caliber. In: Dyck PJ, Thomas PK, Griffin JW, Low PA, Podulso JF, editors. Peripheral neuropathy. 3rd ed. Philadelphia: W.B. Saunders; 1993. p. 389–402.

Hsieh ST, Kidd GJ, Crawford TO, Xu Z, Lin WM, Trapp BD, et al. Regional modulation of neurofilament organization by myelination in normal axons. J Neurosci 1994; 14: 6392–401.

Huxley C, Passage E, Manson A, Putzu G, Figarella-Branger D, Pellisier JF, et al. Construction of a mouse model of Charcot-Marie-Tooth disease type 1A by pronuclear injection of human YAC DNA. Hum Mol Genet 1996; 5: 563–9.

Huxley C, Passage E, Robertson AM, Youl B, Huston S, Manson A, et al. Correlation between varying levels of PMP22 expression and the degree of demyelination and reduction in nerve conduction velocity in transgenic mice. Hum Mol Genet 1998; 7: 449–58.

Kaku DA, Parry GJ, Malamut R, Lupski JR, Garcia CA. Nerve conduction studies in Charcot-Marie-Tooth polyneuropathy associated with a segmental duplication of chromosome 17 [see comments]. Neurology 1993; 43: 1806–8. Comment in: Neurology 1994; 44: 1985–6.

LeGuern E, Gouider R, Mabin D, Tardieu S, Birouk N, Parent P, et al. Patients homozygous for the 17p11.2 duplication in Charcot-Marie-Tooth type 1A disease. Ann Neurol 1997; 41: 104–8.

Low PA. Hereditary hypertrophic neuropathy in the trembler mouse. Part 2. Histopathological studies: electron microscopy. J Neurol Sci 1976; 30: 343–68.

Lupski JR, de Oca-Luna RM, Slaugenhaupt S, Pentao L, Guzzetta V, Trask BJ, et al. DNA duplication associated with Charcot-Marie-Tooth disease type 1A. Cell 1991; 66: 219–32.

Magyar JP, Martini R, Ruelicke T, Aguzzi A, Adlkofer K, Dembic Z, et al. Impaired differentiation of Schwann cells in transgenic mice with increased PMP22 gene dosage. J Neurosci 1996; 16: 5351–60.

Martini R, Zielasek J, Toyka KV, Giese KP, Schachner M. Protein zero (P0)-deficient mice show myelin degeneration in peripheral nerves characteristic of inherited human neuropathies. Nat Genet 1995; 11: 281–6.

Matsunami N, Smith B, Ballard L, Lensch MW, Robertson M, Albertsen H, et al. Peripheral myelin protein-22 gene maps in the duplication in chromosome 17p11.2 associated with Charcot-Marie-Tooth 1A. Nat Genet 1992; 1: 176–9.

Naef R, Suter U. The many facets of the peripheral myelin protein PMP22 in myelination and disease. [Review]. Microsc Res Tech 1998; 41: 359–71.

Nelis E, Van Broeckhoven C, De Jonghe P, Lofgren A, Vandenberghe A, Latour P, et al. Estimation of the mutation frequencies in Charcot-Marie-Tooth disease type 1 and hereditary neuropathy with liability to pressure palsies: a European collaborative study. Eur J Hum Genet 1996; 4: 25–33.

Nicholson GA, Valentijn LJ, Cherryson AK, Kennerson ML, Bragg TL, DeKroon RM, et al. A frame shift mutation in the PMP22 gene in hereditary neuropathy with liability to pressure palsies [published erratum appears in Nat Genet 1994; 7: 113]. Nat Genet 1994; 6: 263–6.

Nukada H, Dyck PJ. Decreased axonal caliber and neurofilaments in hereditary motor and sensory neuropathy, type I. Ann Neurol 1984; 16: 238–41.

Parmantier E, Cabon F, Braun C, D'Urso D, Müller HW, Zalc B. Peripheral myelin protein-22 is expressed in rat and mouse brain and spinal cord motoneurons. Eur J Neurosci 1995; 7: 1080–8.

Patel PI, Lupski JR. Charcot-Marie-Tooth disease: a new paradigm for the mechanism of inherited disease. [Review]. Trends Genet 1994; 10: 128–33.

Patel PI, Roa BB, Welcher AA, Schoener-Scott R, Trask BJ, Pentao L, et al. The gene for the peripheral myelin protein PMP-22 is a candidate for Charcot-Marie-Tooth disease type 1A. Nat Genet 1992; 1: 159–65.

Sanchez I, Hassinger L, Paskevich PA, Shine HD, Nixon RA. Oligodendroglia regulate the regional expansion of axon caliber and local accumulation of neurofilaments during development independently of myelin formation. J Neurosci 1996; 16: 5095–105.

Scherer SS, Xu Y-T, Nelles E, Fischbeck K, Willecke K, Bone LJ. Connexin32-null mice develop demyelinating peripheral neuropathy. Glia 1998; 24: 8–20.

Sereda M, Griffiths I, Puhlhofer A, Stewart H, Rossner MJ, Zimmerman F, et al. A transgenic rat model of Charcot-Marie-Tooth disease. Neuron 1996; 16: 1049–60.

Shy ME, Arroyo E, Sladky J, Menichella D, Jiang H, Xu W, et al. Heterozygous P_0 knockout mice develop a peripheral neuropathy that resembles chronic inflammatory demyelinating polyneuropathy (CIDP). J Neuropathol Exp Neurol 1997; 56: 811–21.

Suh JG, Ichihara N, Saigoh K, Nakabayashi O, Yamanishi T, Tanaka K, et al. An in-frame deletion in peripheral myelin protein-22 gene causes hypomyelination and cell death of the Schwann cells in the new Trembler mutant mice. Neuroscience 1997; 79: 735–44.

Suter U, Snipes GJ. Biology and genetics of hereditary motor and sensory neuropathies. [Review]. Annu Rev Neurosci 1995; 18: 45–75.

Suter U, Welcher AA, Ozcelik T, Snipes GJ, Kosaras B, Francke U, et al. Trembler mouse carries a point mutation in a myelin gene. Nature 1992a; 356: 241–4.

Suter U, Moskow JJ, Welcher AA, Snipes GJ, Kosaras B, Sidman RL, et al. A leucine-to-proline mutation in the putative first transmembrane domain of the 22-kDa peripheral myelin protein in the trembler-J mouse. Proc Natl Acad Sci USA 1992b; 89: 4382–6.

Thomas PK, Marques W Jr, Davis MB, Sweeney MG, King RH, Bradley JL, et al. The phenotypic manifestations of chromosome 17p11.2 duplication. Brain 1997; 120: 465–78.

Timmerman V, Nelis E, Van Hul W, Nieuwenhuijsen BW, Chen KL, Wang S, et al. The peripheral myelin protein gene PMP-22 is contained within the Charcot-Marie-Tooth disease type 1A duplication [published erratum appears in Nat Genet 1992; 2: 84]. Nat Genet 1992; 1: 171–5.

Valentijn LJ, Bolhuis PA, Zorn I, Hoogendijk JE, van den Bosch N, Hensels GW, et al. The peripheral myelin gene PMP-22/GAS-3 is duplicated in Charcot-Marie-Tooth disease type 1A. Nat Genet 1992; 1: 166–70.

Warner LE, Roa BB, Lupski JR. Absence of PMP22 coding region mutations in CMT1A duplication patients: further evidence supporting gene dosage as a mechanism for Charcot-Marie-Tooth disease type 1A. Hum Mutat 1996; 8: 362–5.

Watson DF, Nachtman FN, Kuncl RW, Griffin JW. Altered neurofilament phosphorylation and beta tubulin isotypes in Charcot-Marie-Tooth disease type 1. Neurology 1994; 44: 2383–7.

Wise CA, Garcia CA, Davis SN, Heju Z, Pentao L, Patel PI, et al. Molecular analyses of unrelated Charcot-Marie-Tooth (CMT) disease patients suggest a high frequency of the CMT1A duplication [see comments]. Am J Hum Genet 1993; 53: 853–63. Comment in: Am J Hum Genet 1994; S4: 727–9.

Xu Z, Marszalek JR, Lee MK, Wong PC, Folmer J, Crawford TO, et al. Subunit composition of neurofilaments specifies axonal diameter. J Cell Biol 1996; 133: 1061–9.

Yin X, Crawford TO, Griffin JW, Tu P-H, Lee VM-Y, Li C, et al. Myelin-associated glycoprotein is a myelin signal that modulates the caliber of myelinated axons. J Neurosci 1998; 18: 1953–62.

Young P, Wiebusch H, Stogbauer F, Ringelstein B, Assmann G, Funke H. A novel frameshift mutation in PMP22 accounts for hereditary neuropathy with liability to pressure palsies [see comments]. Neurology 1997; 48: 450–2. Comment in: Neurology 1997; 49: 1478–9.

Zhu Q, Couillard-Després S, Julien J-P. Delayed maturation of regenerating myelinated axons in mice lacking neurofilaments. Exp Neurol 1997; 148: 299–316.

Received December 21, 1998. Revised February 26, 1999. Accepted March 15, 1999